Inspire Create Transform

Wavefield separation cross-correlation imaging condition based on continuous wavelet transform

Juan Guillermo Paniagua C.
M.Sc. in Engineering
PhD (c) in Mathematical Engineering

GRIMMAT - Research group in mathematical modeling

Advisor: PhD Olga Lucía Quintero M.

Outline

Outline

Reverse time migration (RTM)

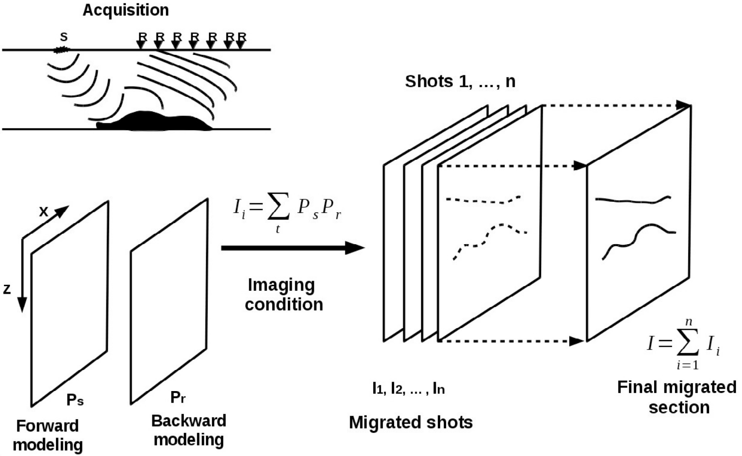

Reverse time migration (RTM)

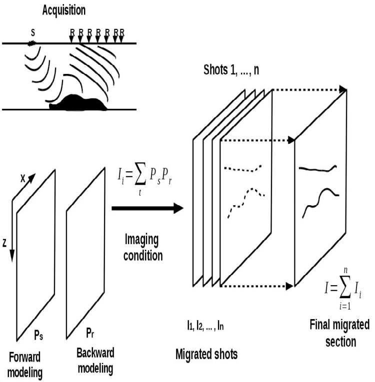

Acoustic wave equation

$$\frac{1}{c(\mathbf{x})^2}\frac{\partial^2 u(\mathbf{x},t)}{\partial t^2} - \nabla^2 u(\mathbf{x},t) = s(\mathbf{x},t)$$

1. Forward propagation of the source wavefield.
2. Backward propagation of the receivers wavefield.
3. Imaging condition.

Reverse time migration (RTM)

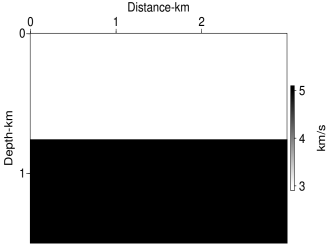

Velocity model

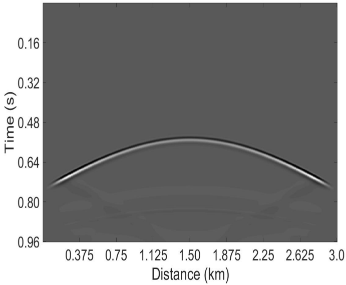

Data recorded

Source wavefield video   Receiver wavefield video

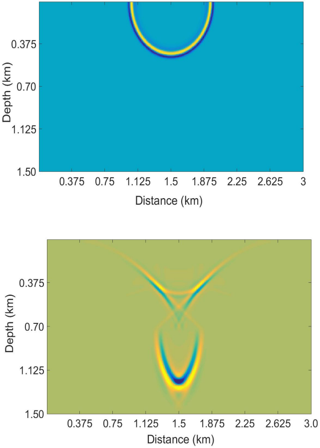
Depth (km)
0.375
0.70
1.125
1.50
0.375 0.75 1.125 1.5 1.875 2.25 2.625 3
Distance (km)
Depth (km)
0.375
0.70
1.125
1.50
0.375 0.75 1.125 1.5 1.875 2.25 2.625 3.0
Distance (km)

$t = 0.20$ s

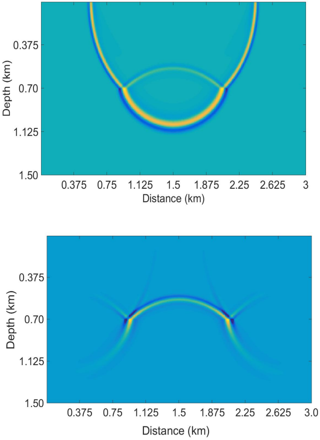
Depth (km)
0.375
0.70
1.125
1.50
0.375 0.75 1.125 1.5 1.875 2.25 2.625 3
Distance (km)
Depth (km)
0.375
0.70
1.125
1.50
0.375 0.75 1.125 1.5 1.875 2.25 2.625 3.0
Distance (km)

$t = 0.36$ s

Zero-lag cross-correlation imaging condition (ZL-CC-IC)

$$I_{cc}(x,z) = \sum_{j=1}^{s_{max}} \sum_{i=1}^{t_{max}} S(x,z;t_i;s_j)R(x,z;t_i;s_j) \tag{1}$$

S: Source wavefield
R: Receiver wavefield
z: Depth
x: Distance
t: Time
t_{max}: Maximum time
s_{max}: Maximum number of sources

Cross-correlation image

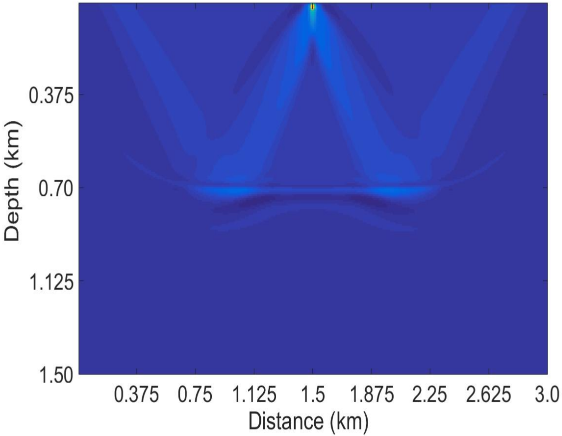

Cross-correlation image

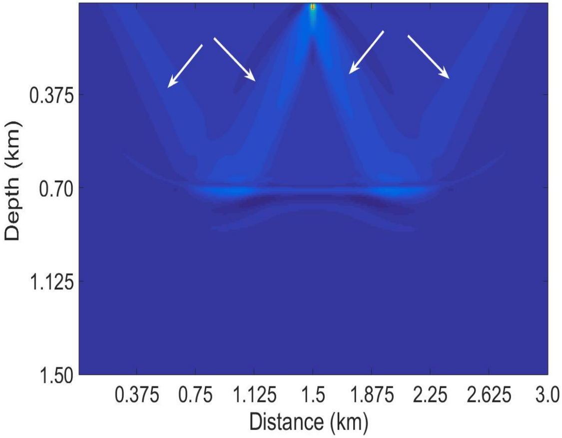

Some wave paths of the wavefield [22]

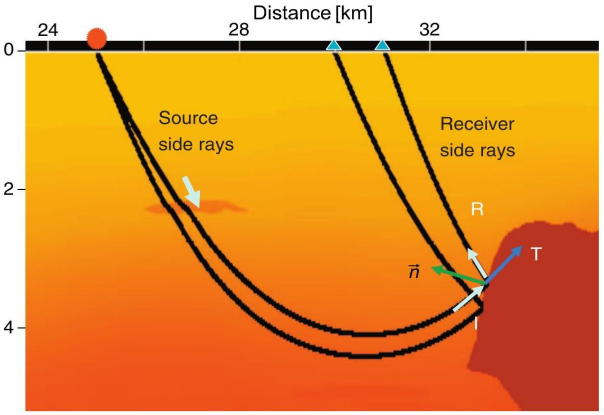

Methods to eliminate the artifacts

- Wavefield propagation approaches ([25, 3, 12]).
- Imaging condition approaches ([38, 20, 17, 22, 43, 31, 35]).
- Post-imaging condition approaches ([45, 16]).

Laguerre-Gauss transform

The Laguerre-Gauss transform of $I(x, y)$ is given by ([41, 15])

$$\tilde{I}(x, y) = \int_{-\infty}^{\infty} \int_{-\infty}^{\infty} LG(f_x, f_y) I(f_x, f_y) e^{2\pi i (f_x x + f_y y)} df_x df_y$$

Where

$$LG(x, y) = (i\pi^2 \omega^4)(x + iy) e^{-\pi^2 \omega^2 (x^2 + y^2)}$$

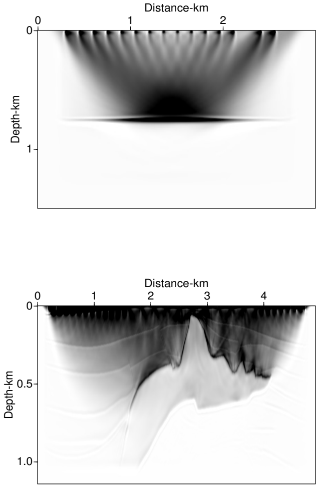

Cross-correlation image

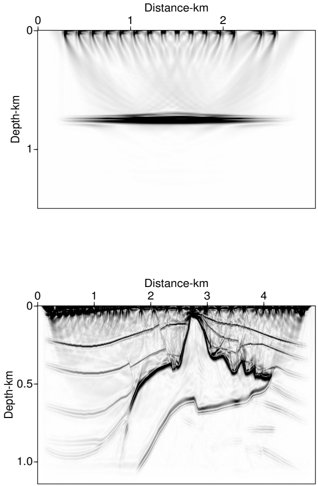

Laguerre-Gauss image

Wavefield decomposition

Taking into account (1)

$$I_{cc}(x,z) = \sum_{j=1}^{s_{max}} \sum_{i=1}^{t_{max}} S(x,z;t_i;s_j) R(x,z;t_i;s_j)$$

$S(x,z;t_i;s_j)$ and $R(x,z;t_i;s_j)$ can be partitioned mathematically as

$$S(x,z;t_i;s_j) = S_d(x,z;t_i;s_j) + S_u(x,z;t_i;s_j)$$

$$R(x,z;t_i;s_j) = R_d(x,z;t_i;s_j) + R_u(x,z;t_i;s_j)$$

Wavefield decomposition

Then, (1) can be expressed as follows

$$
\begin{aligned}
I_{cc}(x,z) = \; & \sum_{j=1}^{s_{max}} \sum_{i=1}^{t_{max}} (S_d(x,z;t_i;s_j)R_u(x,z;t_i;s_j) \\
& +S_u(x,z;t_i;s_j)R_d(x,z;t_i;s_j) \\
& +S_d(x,z;t_i;s_j)R_d(x,z;t_i;s_j) \\
& +S_u(x,z;t_i;s_j)R_u(x,z;t_i;s_j))
\end{aligned}
$$

Then

$$
I_{cc}(x,z) = I_{cc}^{du}(x,z) + I_{cc}^{ud}(x,z) + I_{cc}^{dd}(x,z) + I_{cc}^{uu}(x,z) \quad (2)
$$

Wavefield decomposition

From (2)

$$I_{cc}(x,z) = I_{cc}^{du}(x,z) = \sum_{j=1}^{s_{max}} \sum_{i=1}^{t_{max}} S_d(x,z;t_i;s_j) R_u(x,z;t_i;s_j) \quad (3)$$

$S_d(x,z;t_i;s_j)$: Downgoing source wavefield.
$R_u(x,z;t_i;s_j)$: Upgoing receiver wavefield.

Eq. (3) is exactly what one will get in a one way wave equation migration

Continuous wavelet transform

A wavelet is a function $\psi \in L^2(\mathbb{R})$ with finite energy ([27]), that is,

$$C_\psi = \int_0^\infty \frac{|\hat{\psi}(\omega)|^2}{\omega} d\omega < \infty$$

$\hat{\psi}(\omega)$ is the Fourier transform of $\psi(t)$ given by

$$\hat{\psi}(\omega) = \int_{-\infty}^{\infty} \psi(t) e^{-i2\pi\omega t} dt$$

C_ψ is called the admissibility condition.

Continuous wavelet transform

It is normalized $||\psi|| = 1$ and satisfies the condition that is rapidly decreasing

$$\int_{-\infty}^{\infty} (1 + |t|)|\psi(t)|dt < \infty$$

with zero average and centered in the neighborhood of $t = 0$

$$\int_{-\infty}^{\infty} \psi(t)dt = 0$$

Continuous wavelet transform

Family of wavelets

$$\psi_{s,u}(t) = \frac{1}{\sqrt{s}}\psi\left(\frac{t-u}{s}\right),\ s,u \in \mathbb{R},\ a \neq 0$$

s: Scaling parameter
u: Translation parameter
ψ: Mother wavelet

If $\psi \in L^2(\mathbb{R})$, then $\psi_{s,u}(t) \in L^2(\mathbb{R})$ for all s, u and $||\psi_{s,u}|| = 1$.

Continuous wavelet transform

The integral transformation W_f defined on $L^2(\mathbb{R})$ by

$$W_f(u,s) = \langle f(t), \psi_{s,u}(t) \rangle = \frac{1}{\sqrt{s}} \int_{-\infty}^{\infty} f(t)\psi^* \left(\frac{t-u}{s} \right) dt$$

is called a continuous wavelet transform of $f(t)$.

Gaussian wavelet

$$\psi_n(t) = c_n \frac{d^n}{dt^n} \left(e^{-\frac{t^2}{2}} \right), \ \hat{\psi}_n(\omega) = c_n (i\omega)^n e^{-\frac{\omega^2}{4}}$$

Continuous wavelet transform

The continuous wavelet transform can be expressed as a convolution product

$$W_f(u, s) = \frac{1}{\sqrt{s}} \int_{-\infty}^{\infty} f(t)\psi^* \left(\frac{t-u}{s} \right) dt = f(t) \star \bar{\psi}_s(u)$$

with

$$\bar{\psi}_s(t) = \frac{1}{\sqrt{s}} \psi^* \left(\frac{-t}{s} \right)$$

and the Fourier transform of $\bar{\psi}_s(t)$ is

$$\hat{\bar{\psi}}_s(\omega) = \sqrt{s}\hat{\psi}^*(s\omega)$$

Source wavefield analysis

Algorithm for time-scale analysis of source wavefield

- From the source wavefield $S(x, z, t)$, select for each x the wavefield $S_x(z, t)$.

Source wavefield analysis

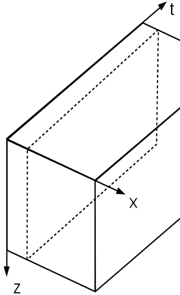

$S(x, z, t)$ wavefield

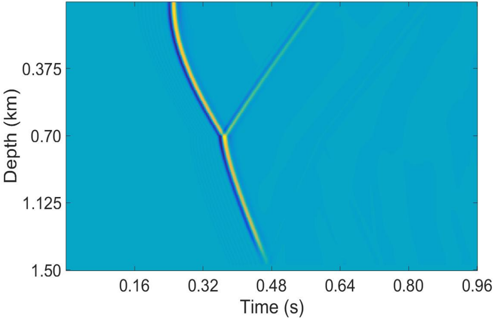

$S_x(z, t)$ at $x = 0.90$ km

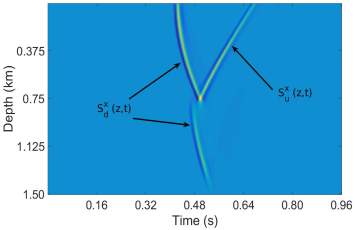

a) $x = 0.375$ km

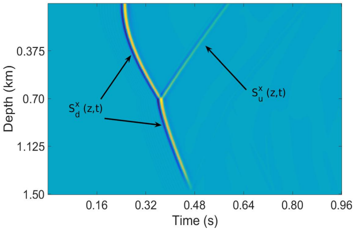

b) $x = 0.90$ km

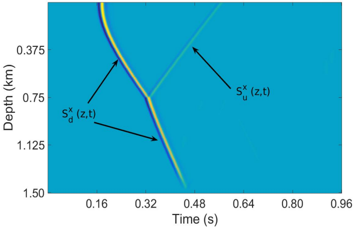

c) $x = 1.125$ km

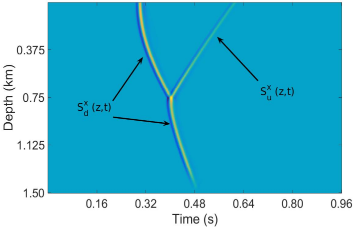

d) $x = 2.25$ km

Source wavefield analysis

Algorithm for time-scale analysis of source wavefield

- From the source wavefield $S(x, z, t)$, select for each x the wavefield $S_x(z, t)$.
- Apply $1D$ CWT on $S_x(z, t)$ along t axis for each z $(S_{x,z}(t))$.

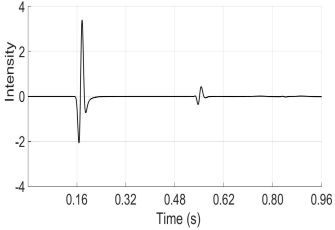

$S_{x=1.125,z}(t)$ at $z = 0$ km

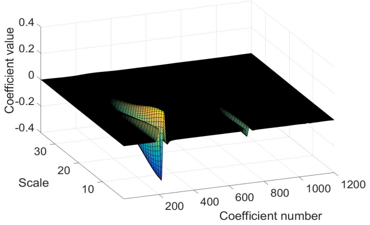

Coefficients of CWT

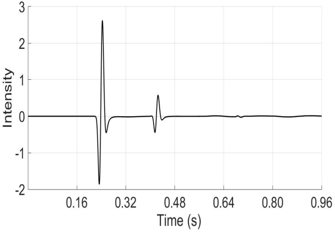

$S_{x=1.125,z}(t)$ at $z = 0.45$ km

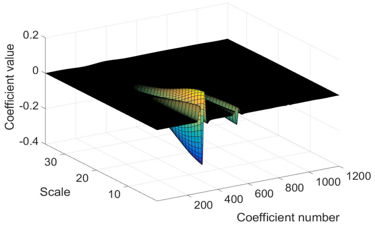

Coefficients of CWT

Source wavefield analysis

Algorithm for time-scale analysis of source wavefield

- From the source wavefield $S(x, z, t)$, select for each x the wavefield $S_x(z, t)$.
- Apply $1D$ CWT on $S_x(z, t)$ along t axis for each z ($S_{x,z}(t)$).
- Select the minimum value of the all coefficients and locate it in $S_{x,z}(t)$ and saved in a new wavefield $S_{x,z}^{new}(t)$. Two more points were taken before and after this point to improve the accuracy.

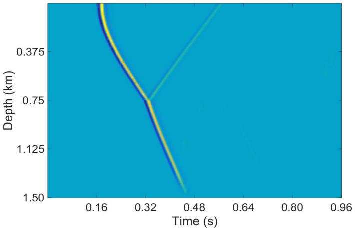

$S_x(z,t)$ at $x = 1.125$ km

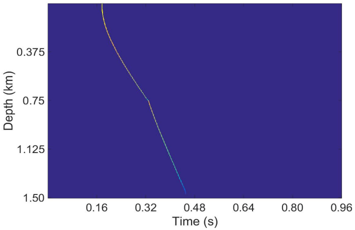

$S^{new}_{x,z}(t)$ at $x = 1.125$ km

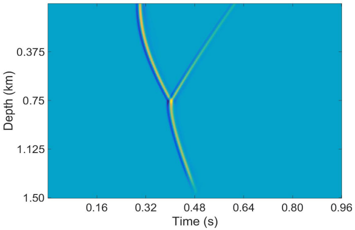

$S_x(z,t)$ at $x = 2.25$ km

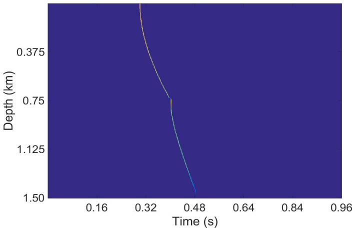

$S^{new}_{x,z}(t)$ at $x = 2.25$ km

Source wavefield analysis

$S(x, z, t)$ wavefield video   Separated $S(x, z, t)$ video

Receiver wavefield analysis

Algorithm for time-scale analysis of receiver wavefield

- From the receiver wavefield $R(x, z, t)$, select for each x the wavefield $R_x(z, t)$.

Receiver wavefield analysis

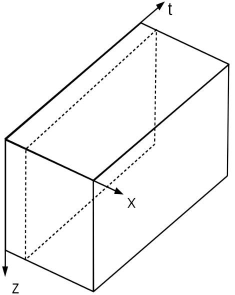

$R(x, z, t)$ wavefield

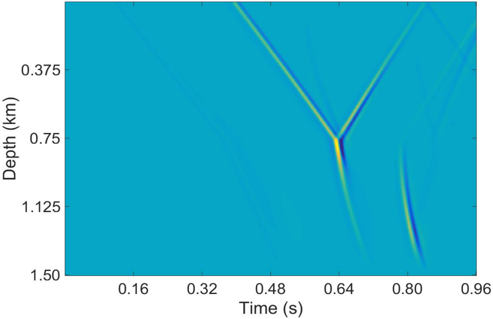

$R_x(z, t)$ at $x = 1.125$ km

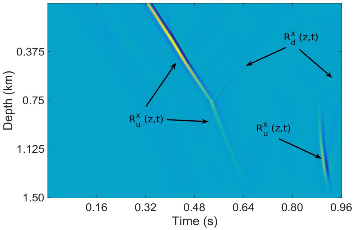

a) $x = 0.675$ km

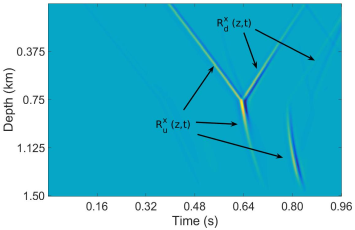

b) $x = 1.125$ km

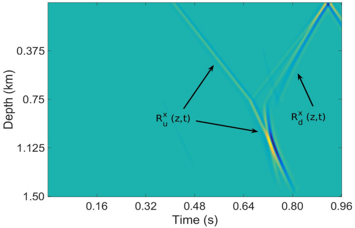

c) $x = 1.50$ km

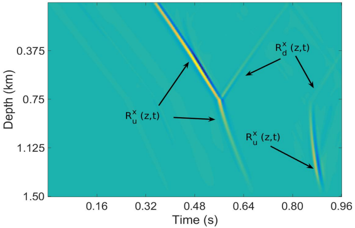

d) $x = 2.25$ km

Receiver wavefield analysis

Algorithm for time-scale analysis of receiver wavefield

- From the receiver wavefield $R(x, z, t)$, select for each x the wavefield $R_x(z, t)$.
- Apply $1D$ CWT on $R_x(z, t)$ along z axis for each t ($R_{x,t}(z)$).

Receiver wavefield analysis

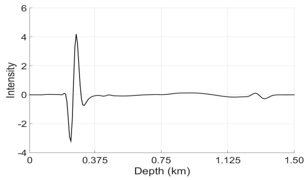

$R_{x=1.125,t}(z)$ at $t = 0.48$ s

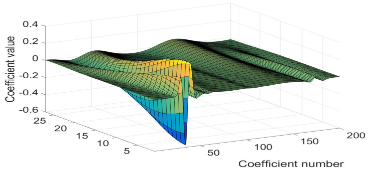

Coefficients of CWT

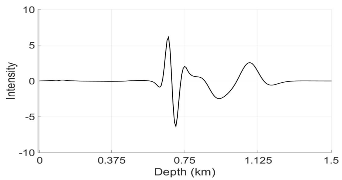

$R_{x=1.125,t}(z)$ at $t = 0.66$ s

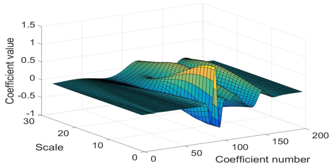

Coefficients of CWT

Receiver wavefield analysis

Algorithm for time-scale analysis of receiver wavefield

- From the receiver wavefield $R(x, z, t)$, select for each x the wavefield $R_x(z, t)$.
- Apply $1D$ CWT on $R_x(z, t)$ along z axis for each t ($R_{x,t}(z)$).
- Select the maximum absolute value of coefficients that co-rresponds to a coefficient with negative value and locate it in $R_{x,t}(z)$ and saved in a new wavefield $R^{new}_{x,t}(z)$. Two more points were taken before and after this point to improve the accuracy.

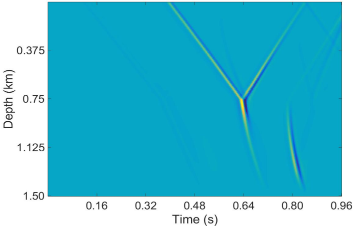

$R_x(z,t)$ at $x = 1.125$ km

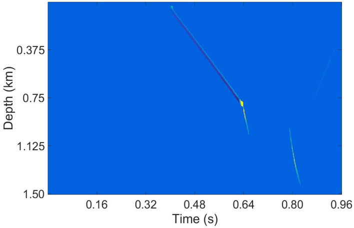

$R_{x,t}^{new}(z)$ at $x = 1.125$ km

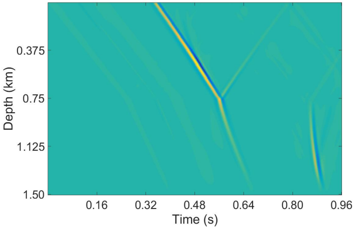

$R_x(z,t)$ at $x = 2.25$ km

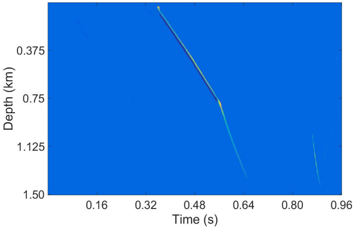

$R_{x,t}^{new}(z)$ at $x = 2.25$ km

Receiver wavefield analysis

Receiver wavefield video   Separated $R(x, z, t)$ video

Separated source and receiver wavefields

Separated $S(x,z,t)$ video   Separated $R(x,z,t)$ video

Cross-correlation image

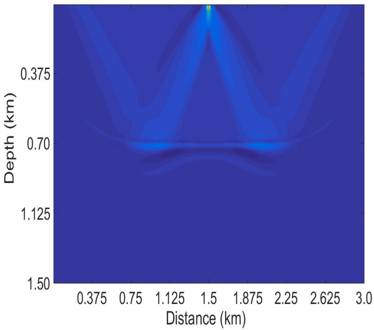

Conventional cross-correlation image

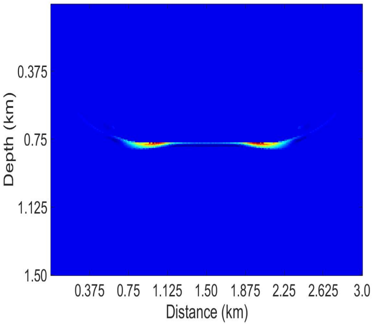

Wavefield separation cross-correlation image

Cross-correlation image

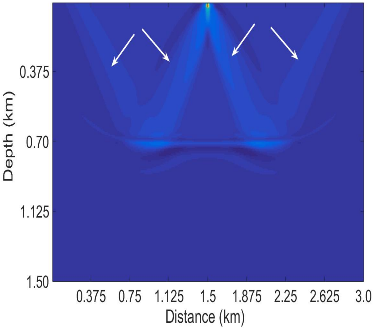

Conventional cross-correlation image

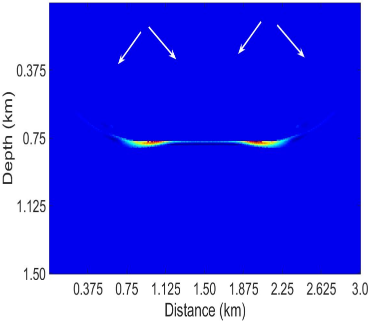

Wavefield separation cross-correlation image

Other synthethic models

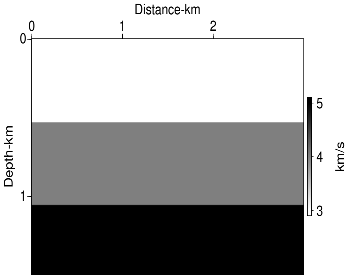

Three-layer model

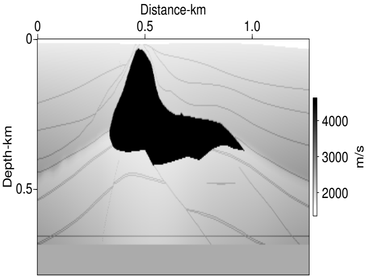

Small salt model

Three-layer model

$S(x, z, t)$ video   Separated $S(x, z, t)$ video

Three-layer model

$R(x, z, t)$ video   Separated $R(x, z, t)$ video

Three-layer model

Cross-correlation image

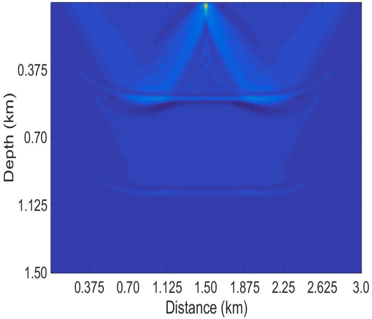

Conventional ZL-CC-IC

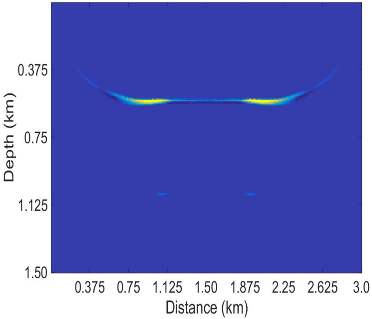

ZL-CC-IC with separated wavefield

Three-layer model

Receiver wavefield analysis

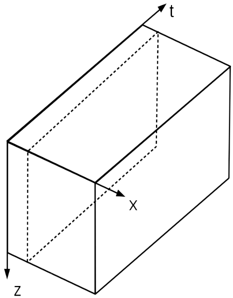

$R(x, z, t)$

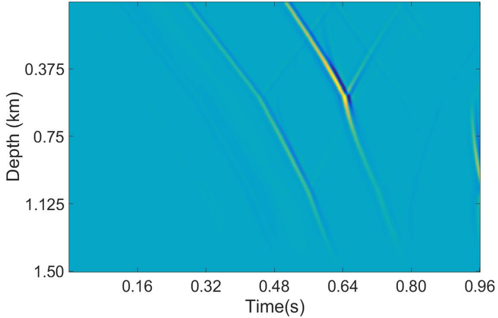

$R(x, z, t)$ at $x = 0.9$ km

Three-layer model

Receiver wavefield analysis

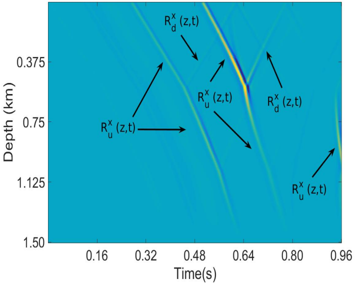

$R(x, z, t)$ at $x = 0.9$ km

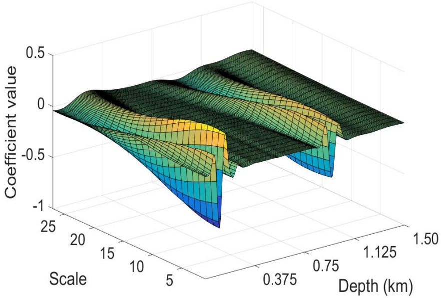

Coefficients CWT $R(x = 0.9, z, t)$ at $t = 0.54$ s

Wavelet transform modulus maxima (WTMM)

WTMM corresponds to the entire set of local maximum points of the absolute value of wavelet transform.

$$WTMM = \left\{ (u_0, s_0) \in (\mathbb{R}, \mathbb{R}^+), \left. \frac{\partial |W_f(u,s)|}{\partial u} \right|_{u=u_0, s=s_0} = 0 \right\}$$

The set of points of the WTMM concatenated through scales are known as maximum lines.

Wavelet transform modulus maxima (WTMM)

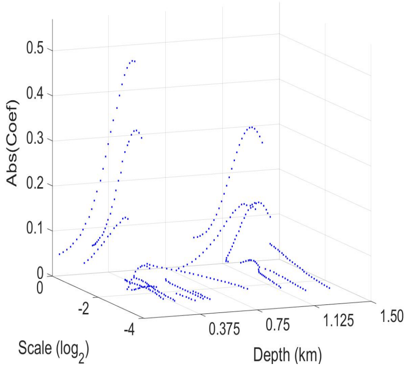

Local maximum points

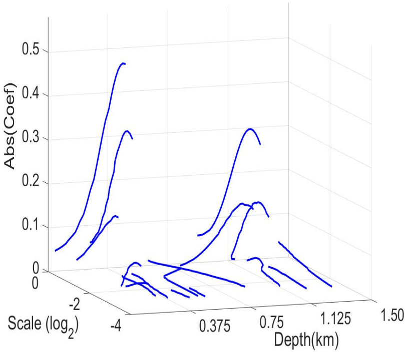

Maximum lines chaining

Three-layer model

Cross-correlation image

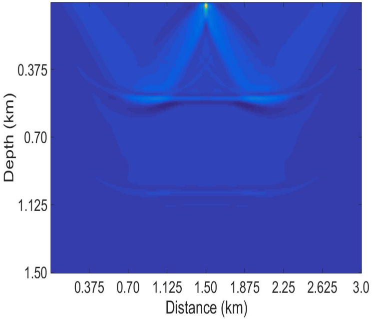

Conventional ZL-CC-IC

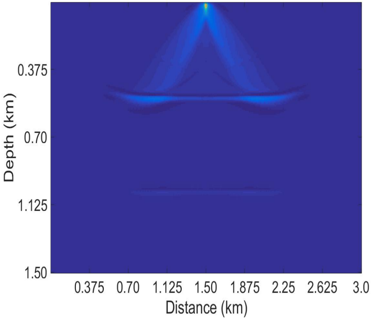

ZL-CC-IC with separated source wavefield

Small salt model

$S(x, z, t)$ video   Separated $S(x, z, t)$ video

Small salt model

Cross-correlation image

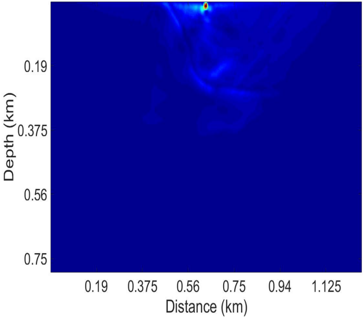

Conventional ZL-CC-IC

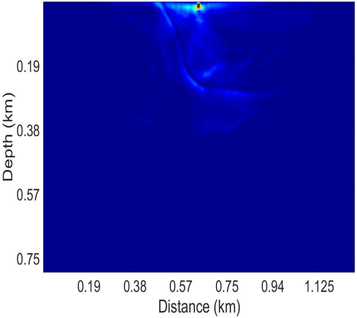

ZL-CC-IC with separated source wavefield

Preliminary results

Paniagua, J.G. and Quintero, O.L., 2017, Attenuation of reverse time migration artifacts using Laguerre-Gauss filtering. Poster accepted in 79th EAGE Conference & Exhibition 2017, Paris.

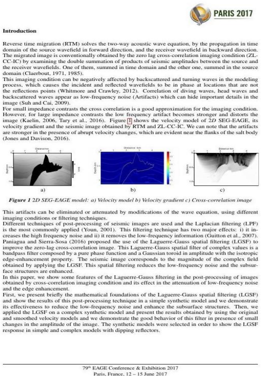

PARIS 2017

Introduction

Reverse time migration (RTM) solves the two-way acoustic wave equation, by the propagation in time domain of the source wavefield in forward direction, and the receiver wavefield in backward direction. The migrated image is conventionally obtained by the zero lag cross-correlation imaging condition (ZL-CC-IC) by examining the double summation of products of seismic amplitudes between the source and the receiver wavefields. One of them, summed in time domain and the other one, summed in the source domain (Claerbout, 1971, 1985).

This imaging condition can be negatively affected by backscattered and turning waves in the modeling process, which causes the incident and reflected wavefields to be in phase at locations that are not the reflections points (Whitmore and Crawley, 2012). Correlation of diving waves, head waves and backscattered waves appear as low-frequency noise (Artifacts) which can hide important details in the image (Suh and Cai, 2009).

For small impedance contrasts the cross correlation is a good approximation for the imaging condition. However, for large impedance contrasts the low frequency artifact becomes stronger and distorts the image (Kaelin, 2006, Tary et al., 2016). Figure 1 shows the velocity model of 2*D* SEG-EAGE, its velocity gradient and the seismic image obtained by RTM and ZL-CC-IC. We can note that the artifacts are stronger in the presence of abrupt velocity changes, which are evident near the flanks of the salt body (Jones and Davison, 2016).

a) b) c)

***Figure 1** 2D SEG-EAGE model: a) Velocity model b) Velocity gradient c) Cross-correlation image*

This artifacts can be eliminated or attenuated by modifications of the wave equation, using different imaging conditions or filtering techniques.

Different techniques of post-processing of seismic images are used and the Laplacian filtering (LPF) is the most commonly applied (Youn, 2001). This filtering technique has two major effects: i) it increases the high frequency noise and ii) it removes the low-frequency information (Guitton et al., 2007). Paniagua and Sierra-Sosa (2016) proposed the use of the Laguerre-Gauss spatial filtering (LGSF) to improve the zero-lag cross-correlation image. This Laguerre-Gauss spatial filter of complex values is a bandpass filter composed by a pure phase function and a Gaussian toroid in amplitude with the isotropic edge-enhancement property. The seismic image corresponds to the magnitude of the complex field obtained by applying the LGSF. This spatial filtering reduces the low-frequency noise and the subsurface structures are enhanced.

In this paper, we show some features of the Laguerre-Gauss filtering in the post-processing of images obtained by cross-correlation imaging condition and its effect in the attenuation of low-frequency noise and the edge enhancement.

First, we present briefly the mathematical foundations of the Laguerre-Gauss spatial filtering (LGSF) and show the results of this post-processing technique in a simple synthetic model and we demonstrate its effectiveness to reduce the low-frequency noise and enhance the subsurface structures. Then, we applied the LGSF on a complex synthetic model and present the results obtained by using the original and smoothed velocity models and we demonstrate the good behavior of this filter in presence of small changes in the amplitude of the image. The synthetic models were selected in order to show the LGSF response in simple and complex models with dipping reflectors.

79th EAGE Conference & Exhibition 2017
Paris, France, 12 – 15 June 2017

Preliminary results

Paniagua, J.G. and Quintero, O.L., 2017, The use of Laguerre-Gauss transform in 2D reverse time migration imaging. Paper accepted in 15th International Congress of the Brazilian Geophysical Society and the EXPOGEf 2017, Rio de Janeiro.

The use of Laguerre-Gauss transform in 2D reverse time migration imaging

Juan Guillermo Paniagua (*), Universidad EAFIT, Olga Lucía Quintero, Universidad EAFIT

Copyright 2017, SBGf - Sociedade Brasileira de Geofísica

This paper was prepared for presentation during the 15th International Congress of the Brazilian Geophysical Society held in Rio de Janeiro, Brazil, 31 July to 3 August, 2017.

Contents of this paper were reviewed by the Technical Committee of the 15th International Congress of the Brazilian Geophysical Society and do not necessarily represent any position of the SBGf, its officers or members. Electronic reproduction or storage of any part of this paper for commercial purposes without the written consent of the Brazilian Geophysical Society is prohibited.

Abstract

Zero-Lag Cross-Correlation Imaging condition (ZL-CC-IC) is widely used in Reverse Time Migration (RTM) for the recovery of structural images of the subsurface. The presence of spatial low frequency noise so called artifacts, is one of the challenges of post processing in certain complex velocity field models with special features. Paniagua and Sierra-Sosa (2016) proposed a new post processing technique for the edge enhancement and reduction of low frequency artifacts; now our aim is to demonstrate the good performance of this technique and establish quantitative features and relations between the numerical results and the physical phenomenon. We present a comparative spectral study of the zero-lag cross-correlation imaging condition (ZL-CC-IC), zero-lag cross-correlation plus Laplacian filtering (ZL-CC-LP) and zero-lag cross-correlation plus Laguerre-Gauss filtering (ZL-CC-LG) showing their frequency features, also we show some results of the Laguerre-Gauss filtering applied in complex synthetic datasets and finally, using a smoothed velocity model in order to simulate the uncertainties of a real application, we show the good results obtained by using the Laguerre-Gauss Filtering posterior to RTM.

Introduction

The imaging condition in reverse time migration (RTM) has been conventionally obtained by the zero lag cross-correlation (ZL-CC) by examining the double summation of products of seismic amplitudes between the source and the receiver wavefields. One of them, summed in time domain and the other one, summed in the source domain. (Claerbout, 1971, 1985). This imaging condition is kinematically accurate at the reflectors due to the fact that incident and reflected wavefields are coincident in space and time (Liu, et al., 2011), but the migrated amplitudes no longer hold any physical meaning. It produces kinematically correct images of the geometry of the subsurface structure (Chattopadhay and McMechan, 2008).

However, the image is contaminated with low spatial frequency noise (Artifacts) due to the unwanted cross-correlation of diving waves, head waves and backscattered waves (Suh and Cai, 2009).

For small impedance contrasts the cross correlation is a good approximation for the imaging condition. However, for large impedance contrasts the low frequency artifact becomes stronger and distorts the image (Kaelin, 2006, Tary et al., 2016). In presence of strong velocity changes, strong amplitude changes occur and the appearance of artifacts is greater than in smooth velocity changes (Loewenthal et al, 1987).

Different techniques have been proposed to eliminate or reduce the low frequency noise, which can be classified in: i) wavefield propagation approaches (wave equation is modified), ii) imaging condition approaches (reflection energy is kept in the final image) and iii) post-imaging condition approaches (image is filtered) (Guitton et al., 2007).

In regard to the latter, the Laplacian filtering is the post-processing technique frequently used to attenuate the low frequency artifacts present in the structural image obtained through ZL-CC-IC but it increases the high frequency noise in the image (Guitton et al., 2007). Looking for a new technique that allows for the enhancement of the structural images obtained in RTM, Paniagua and Sierra-Sosa (2016) proposed the use of the Laguerre-Gauss transform in the post-processing of the image obtained by zero-lag cross-correlation imaging condition (ZL-CC-IC). The kernel of this transformation is called the Laguerre-gauss filter and it consists in a pure-phase function that is composed by a heavy-side function with a π gap when crossing the origin in every angular direction and in the amplitude is a Gaussian toroid. With this spatial bandpass filter, the low-frequency noise (artifacts) is reduced and the subsurface structures are more defined. This filter enhances the edges without resolution loss.

It is important to demonstrate that as post processing strategy, the Laguerre-Gauss filtering (ZL-CC-LG) improves the images obtained even in complex structures and the high frequency noise is also removed, enhancing the capability of interpretation. Also, by featuring the frequency spectrum allows for the quantification of the advantages to be used in a future research.

In this paper, we show some spectral features of the Laguerre-Gauss filtering in the post-processing of seismic images obtained by the conventional zero-lag cross-correlation imaging condition and the good performance of this filter in the edge enhancement and reduction of low frequency artifacts.

First, we compare and analyze the Fourier spectra obtained by the spatial 2D fast Fourier transform of the images obtained by the zero-lag cross-correlation (ZL-CC-IC), zero-lag cross-correlation plus Laplacian filtering (ZL-CC-LP) and zero-lag cross-correlation plus Laguerre-Gauss filtering (ZL-CC-LG). Second, we show some results of the Laguerre-Gauss filtering applied in synthetic datasets and finally, using some smoothed velocity

Fifteenth International Congress of the Brazilian Geophysical Society

Preliminary results

Paniagua, J.G., Sierra-Sosa, D and Quintero, O.L., 2017, Laguerre-Gauss filters in reverse time migration image reconstruction. Scientific paper submitted to Revista Brasileira de Geofísica.

LAGUERRE-GAUSS FILTERS IN REVERSE TIME MIGRATION IMAGE RECONSTRUCTION

Juan Guillermo Paniagua, Daniel Sierra-Sosa and Olga Lucía Quintero

ABSTRACT

Reverse time migration (RTM) solves the acoustic or elastic wave equation by means of the extrapolation from source and receiver wavefield in time. A migrated image is obtained by applying a criteria known as imaging condition. The cross-correlation between source and receiver wavefields is the commonly used imaging condition. However, this imaging condition produces spatial low-frequency noise, called artifacts, due to the unwanted correlation of the diving, head and backscattered waves. Several techniques have been proposed to reduce the artifacts occurrence. Derivative operators as Laplacian are the most frequently used. In this work, we propose a technique based on a spiral phase filter ranging from 0 to 2π, and a toroidal amplitude bandpass filter, known as Laguerre-Gauss transform. Through numerical experiments we present the application of this particular filter on three synthetic data sets. In addition, we present a comparative spectral study of images obtained by the zero-lag cross-correlation imaging condition, the Laplacian filtering and the Laguerre-Gauss filtering, showing their frequency features. We also present evidences not only with simulated noisy velocity fields but also by comparison with the model velocity field gradients that this method improves the RTM images by reducing the artifacts and notably enhance the reflective events.

Keywords: Laguerre-Gauss transform, zero-lag cross-correlation, seismic migration, imaging condition.

FILTROS DE LAGUERRE-GAUSS EM IMPRESSÃO DE IMAGEM DE MIGRAÇÃO DE TEMPO INVERSO

RESUMO

A migração reversa no tempo (RTM) resolve a equação de onda acústica ou elástica por meio da extrapolação a partir do campo de onda da fonte e do receptor no tempo. Uma imagem migrada é obtida aplicando um critério conhecido como condição de imagem. A correlação cruzada entre campos de onda de fonte e receptor é a condição de imagem comumente usada. No entanto, esta condição de imagem produz ruído espacial de baixa frequência, chamados artefactos, devido à correlação indesejada das ondas de mergulho, cabeça e retrodifusão. Várias técnicas têm sido propostas para reduzir a ocorrência de artefatos. Operadores derivados como Laplaciano são os mais utilizados. Neste trabalho, propomos uma técnica baseada em um filtro de fase espiral que varia de 0 a 2π, e um filtro passa-banda de amplitude toroidal, conhecido como transformada de Laguerre-Gauss. Através de experimentos numéricos, apresentamos a aplicação deste filtro particular em três

1

Preliminary results

Quintero, O.L. and Paniagua, J.G., 2017, Singularity analysis of receiver field and its relation to RTM imaging condition. Paper to be submitted in an indexed journal.

ECOPETROL	ESTRUCTURA DE ARTÍCULO CT&F		
	GESTIÓN DE TECNOLOGÍA DE NEGOCIO DIRECCIÓN ESTRATÉGICA DE INNOVACIÓN, CONOCIMIENTO Y TECNOLOGÍA		
	GTN-F-008	Elaborado 03/10/2013	Versión 3

Análisis de singularidad del campo receptor y su relación con la condición de imagen en RTM

Singularity analysis of receiver field and its relation to RTM Imaging condition

O.L Quintero M [1], Juan Guillermo Paniagua C.[2],

[1] Grupo de Investigación en Modelado Matemático, Escuela de Ciencias Universidad EAFIT. Medellín, Antioquia, Colombia
[2] Estudiante de Doctorado en Ingeniería Matemática, Universidad EAFIT. Medellín, Antioquia, Colombia. Instituto Tecnológico Metropolitano - ITM.

e-mail: oquinte1@eafit.edu.co jpaniagu@eafit.edu.co

(Recibido: Enero 31 de 2017; Aceptado: Mes, día y año)

Abstract: In this paper we introduce the singularity spectrum algorithm of a seismogram and analyze the features time-scale of the traces and the superposition of the scalogram of the complete set of traces, extracting their main features in time-scale domain that provide clues for the possible localization of artifacts that appears by Zero Lag Cross-Correlation imaging condition (ZLCC) of the operator Reverse Time Migration (RTM). We also tested the post-processing of ZLCC by Laplacian Filtering and Laguerre-Gauss Filtering (Paniagua and Sierra, 2016) and compare their localization and artifact removal capabilities in terms of the features found by Singularity Analysis.
Keywords: Wavelet Transform Modulus Maxima, Zero-Lag Cross-Correlation, Laguerre-Gauss Filter, and seismic migration.

Resumen: En este trabajo presentamos el algoritmo de espectro de singularidad de un sismograma y analizamos las características tiempo-escala de las trazas y la superposición del escalograma del conjunto completo de trazas, extrayendo sus rasgos principales en dominio del tiempo-escala que pueden dar claves para la localización de artefactos que aparecen en la condición de imagen por correlación cruzada con cero retraso (Zero-Lag Cross-Correlation) del operador de Migración Tiempo Reverso. También evaluamos el post procesamiento de la imagen obtenida vía condición de imagen por correlación cruzada con cero retraso usando filtrado Laplaciano y el filtrado Laguerre-Gauss (Paniagua and Sierra, 2016) comparando su capacidad de localización y remoción de artefactos en términos de las características encontradas por análisis de singularidad.
Palabras Claves: Transformada Wavelet Módulo Máximo, Zero-Lag Cross-Correlation, Filtro Laguerre-Gauss y Migración sísmica.

INTRODUCTION

Reverse time migration (RTM) is a very well-known technique for the retrieval of images of the subsurface from the solution of the acoustic wave equation for wavefield propagation through a

1/27

Future work

- Analyze and study the extraction of information about the upgoing and downgoing components of source and receiver wavefields obtained through the CWT and WTMM.
- Analyze the features of the coefficients in CWT and WTMM of the signals in order to select and extract the information properly.
- Improve the algorithm to extract the relevant information about source and receiver wavefields in multi-layer synthetic models.
- Apply the proposed method in migrations with multiple shots.

Future work

- Extend the implementation of the algorithm to other complex synthetic models.
- Realize a singularity analysis of wavefields in order to find the relationship between the local maximum points and lines chaining, obtained by CWT and WTMM, with the Hölder exponent. (Our hypothesis is that there is a relationship between the local maximum points and the Hölder exponent)

References

[1] B. Arntsen, B. Kritski, B. Ursin, and L. Amundsen, *Shot-profile amplitude crosscorrelation imaging condition*, Geophysics **78** (2013), no. 4, S221–S231.

[2] Edip Baysal, Dan D. Kosloff, and John W. C. Sherwood, *Reverse time migration*, Geophysics **48** (1983), no. 11, 1514–1524.

[3] Edip Baysal, Dan D. Kosloff, and John W.C. Sherwood, *A two way nonreflecting wave equation*, Geophysics **49** (1984), no. 2, 132–141.

References

[4] B. Biondi, *3-D Seismic Imaging* , Investigations of Geophysics, vol. 14, Society of Exploration Geophysicists, 2006.

[5] Nándor Bokor and Yoshinori Iketaki, *Laguerre-Gaussian radial Hilbert transform for edge-enhancement Fourier transform x-ray microscopy*, Optics Express **19** (2009), no. 7, 5533–5539.

[6] S. Chattopadhyay and G. McMechan, *Imaging conditions for prestack reverse time migration*, Geophysics **73** (2008), no. 3, 81–89.

References

[7] J. F. Claerbout, *Toward a unified theory of reflector mapping*, Geophysics **36** (1971), no. 3, 467–481.

[8] ———, *Imaging the Earth's interior*, Blackwell Scientific Publications, 1985.

[9] M. Cogan, R. Fletcher, R. King, and D. Nichols, *Normalization strategies for reverse-time migration*, SEG Annual meeting Society of Exploration Geophysicists (2011), 3275–3279.

References

[10] J. Costa, F. Silva, R. Alcántara, J. Schleicher, and A. Novais, *Obliquity-correction imaging condition for reverse time migration*, Geophysics **74** (2009), no. 3, S57–S66.

[11] L. Debnath and D. Bhatta, *Integral transforms and their applications*, CRC press, 2010.

[12] R. Fletcher, P. Fowler, and P. Kitchenside, *Suppressing artifacts in prestack reverse time migration*, 75th International Annual Meeting, SEG, Expanded abstracts (2005), 2049–2051.

References

[13] C. Fleury, *Increasing illumination and sensitivity of reverse-time migration with internal multiples* , Geophysical Prospecting **61** (2013), no. 5, 891–906.

[14] I. Freund and V Freilikher, *Parameterization of anisotropic vortices*, Journal of the Optical Society of America A **14** (1997), no. 8, 1902–1910.

[15] C. Gou, Y. Han, and J. Xu, *Radial Hilbert transform with Laguerre-Gaussian spatial filters*, Optics Letters **31** (2006), no. 10, 1394–1396.

References

[16] A. Guitton, B. Kaelin, and B. Biondi, *Least-square attenuation of reverse time migration*, 76th International Annual Meeting, SEG, Expanded abstracts (2006), 2348–2352.

[17] A. Guitton, A. Valenciano, D. Bevc, and J. Claerbout, *Smoothing imaging condition for shot-profile migration*, Geophysics **72** (2007), no. 3, 149–154.

References

[18] M. Haney, L. Bartel, D. Aldridge, and N. Symons, *Insight into the output of reverse time migration: What do the amplitudes mean?*, 75th International Annual Meeting, SEG, Expanded abstracts (2005), 1950–1953.

[19] L. Hu and G. McMechan, *Wave-field transformations of vertical seismic profiles*, Geophysics **52** (1987), 307–321.

[20] B. Kaelin and A. Guitton, *Imaging condition for reverse time migration*, 76th International Annual Meeting and exposition, SEG, Expanded abstracts (2006), 2594–2598.

References

[21] D. Kosloff and E. Baysal, *Migration with the full wave equation*, Geophysics **48** (1983), 677–687.

[22] F. Liu, G. Zhang, S. Morton, and J. Leveille, *An effective imaging condition for reverse time migration using wavefield decomposition*, Geophysics **76** (2011), no. 10, 29.

[23] G. C. Liu, X. H. Chen, J. Y. Song, and Z. H. Rui, *A stabilized least-squares imaging condition with structure constratints*, Applied Geophysics **9** (2012), no. 4, 459–467.

References

[24] D. Loewenthal and Mufti I. , *Reverse time migration in spatial frequency domain*, Geophysics **48** (1983), no. 5, 627–635.

[25] D. Loewenthal, P. Stoffa, and E. Faria, *Suppressing the unwanted reflections of the full wave equation*, Geophysics **52** (1987), no. 7, 1007–1012.

[26] J. R. Macdonald and M. K. Brachman, *Linear-system integral transform relations*, Reviews of modern physics **28** (1956), no. 4, 393–422.

References

[27] S. Mallat, *A wavelet tour of signal processing*, second ed., Academic press, 1999.

[28] G. A. McMechan, *Migration by extrapolation of time - depend boundary values*, Geophysics Prospecting **31** (1983), 413–420.

[29] B Nguyen and G. McMechan, *Excitation amplitude imaging condition for prestack reverse time migration*, Geophysics **78** (2013), no. 1, 37–46.

References

[30] J. G. Paniagua and D. Sierra-Sosa, *Laguerre Gaussian filters in Reverse Time Migration image reconstruction*, VII Simpósio Brasileiro de Geofísica, expanded abstract accepted (2016).

[31] R. Pestana, A. Dos Santos, and E. Araujo, *RTM imaging condition using impedance sensitivity kernel combinated with the Poynting vector*, SEG Technical Program Expanded Abstracts (2014), 3763–3768.

[32] W. K. Pratt, *Digital image processing*, Wiley Interscience, 2001.

References

[33] Y. Qin and R. McGarry, *True-amplitude common-shot acoustuc reverse time migration*, SEG Annual meeting Society of Exploration Geophysicists (2013).

[34] J. Schleicher, J Costa, and A. Novais, *A comparison of imaging for wave-equation shot-profile migration*, Geophysics **73** (2007), no. 6, S219–S227.

[35] J. Shragge, *Reverse time migration from topography*, Geophysics **79** (2014), no. 4, 1–12.

References

[36] C. Stolk, M. De Hoop, and T. Root, *Linearized inverse scattering based on seismic Reverse Time Migration*, Proceedings of the Project Review, Geo-Mathematical imaging group **1** (2009), 91–108.

[37] S. Y. Suh and J. Cai, *Reverse-time migration by fan filtering plus wavefield decomposition*, SEG 2009 International Exposition and Annual Meeting (2009), 2804–2808.

References

[38] A. Valenciano and B. Biondi, *Deconvolution imaging condition for shot profile migration*, 73th International Annual Meeting and exposition, SEG, Expanded abstracts (2003), 1059–1062.

[39] J. C. Van den Berg, *Wavelets in Physics*, Cambridge University Press, 2004.

[40] F. Vivas and R. Pestana, *Imaging condition to true amplitude shot-profile migration: A comparison of stabilization techniques*, 10th International congress ofnthe Barazilian Geophysical Society (2007), 1668–1672.

References

[41] W. Wang, T. Yokozeki, R. Ishijima, M. Takeda, and S. G. Hanson, *Optical vortex metrology based on the core structures of phase singularities in Laguerre-Gauss transform of a speckle pattern*, Optics Express **14** (2006), no. 22, 10195–10206.

[42] Z. Wang, H. Ding, G. Lu, and X. Bi, *Reverse-tiome migration based optical imaging*, IEEE Transactions on medical imaging **35** (2016), no. 1, 273–281.

References

[43] N. Whitmore and S. Crawley, *Applications of RTM inverse scattering imaging conditions*, 82nd Annual International Meeting, SEG, Expanded abstracts (2012), 779–784.

[44] K. Yoon and K. Marfurt, *Reverse time migration using the Poynting vector*, Exploration Geophysics **37** (2006), 102–107.

[45] O. Youn and H. Zhou, *Depth imaging with multiples*, Geophysics **66** (2001), no. 11, 246–255.

[46] M. S. Zhdanov, *Geophysical inverse theory and regularization problems*, Elseiver, 2002.